Molecular design targets and optimization of low-temperature thermal desalination systems

Alejandro Garciadiego[a], Tengfei Luo[b], Alexander W. Dowling[a,*]

[a] *Department of Chemical and Biomolecular Engineering*
[b] *Department of Aerospace and Mechanical Engineering*
University of Notre Dame, Notre Dame, IN 46556

Abstract

Directional solvent extraction (DSE) is an emerging membrane-free liquid-liquid extraction process to desalinate water using low-grade heat. Several unique features make DSE a potentially disruptive desalination technology: 1) it is thermally driven and utilizes low-grade heat; 2) it does not require the use of membranes; 3) there are opportunities to intensify, modularize and customize the process; 4) there is a vast solvent molecular design space. This work establishes a technoeconomic modeling framework to simultaneous optimize and heat integrate the DSE process. We perform rapid bottom-up screening to predict the energy intensity levelized cost of water (LCOW) of organic acid and ionic liquid directional solvents (DS) in an optimized DSE process. Likewise, we perform top-down analysis to set continuous solvent property targets necessary to realize a LCOW of less than $\$0.5/m^3$. LCOW is most sensitive to the solubility of the DS in water and thermoresponsive ability (a.k.a. yield) of the solvent, i.e., the change in the solubility of water in the DS with temperature. Despite their lower cost, organic acids have a small thermoresponsive ability and LCOW of at least $\$1.3/m^3$. In contrast, we set modest quantitative thermophysical property targets for ionic liquid DS to achieve below $\$0.5/m^3$ LCOW.

*Corresponding author
Email address: adowling@nd.edu (Alexander W. Dowling)

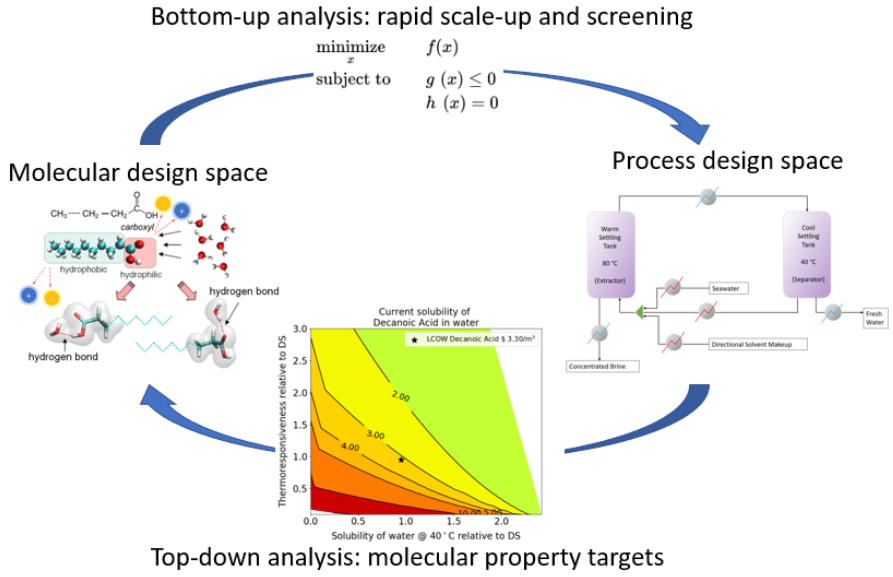

Graphical abstract

Keywords: thermal desalination, liquid-liquid extraction, technoeconomic optimization, levelized cost of water, heat integrations, ionic liquids

1. Highlights

- Directional solvent extraction (DSE) is a potentially transformative low-grade heat renewable desalination technology
- Created a technoeconomic optimization framework for DSE with embedded heat integration and identified the most important solvent thermophysical properties
- Determined fatty acid directional solvents are unable to meet \$0.50/m^3 levelized cost of water (LCOW) goal due to inadequate solvent thermophysical properties
- Set quantitative solvent thermophysical property targets for ionic liquid directional solvents to achieve less than \$0.50/m^3 LCOW goal

2. Introduction

Water consumption is critical to modern society; the average American family uses approximation 1140 liters of municipal water per day [1], and 130 million Americans face severe water scarcity at least part of the year [2]. Globally, 3.8 billion people currently experience water scarcity [3], and it is estimated that 66% of the world's population could be living under water-stressed conditions by 2025 [4]. Although the costs of water obtained from desalination have fallen in the last decade, they are higher than obtaining freshwater from rivers, groundwater, or water recycling. In 2015, less than one percent of the water consumed globally was produced by desalination [5].

The expansion of oil and gas extraction in the US has created new water and environmental challenges [1]. In 2012, 3.57 billion m^3 of produced water was extracted in the US. In the Delaware Basin, up to 4 barrels of water are produced per barrel of oil [6]; to put this number in perspective, around 0.50 liters of produced water may be generated to supply energy for one hour in an average American household. The salinity of produced water is typically 35,000 ppm to 300,000 ppm, which may be up to eight times higher than seawater salinity (35,000 ppm) [7]. Unfortunately, current desalination technologies are unpractical to treat such high salinity brines [8]. Large water volumes (about 20,000 m^3 on average per well) from oil and gas production also remain challenging, even after water supply chain optimization. [9, 10]. There is a pressing need and opportunity for new technologies to treat produced water.

There is no one-size-fits-all technology for water treatment. Instead, there is a growing emphasis on fit-for-purpose treatment in decentralized networks [12]. In this paradigm, water is treated to only the specifications needed for specific end uses. Table 1 highlights different water quality levels (salinity), appropriate end uses, and candidate desalination technologies. While evaporative and reverse osmosis desalination technologies are commonly deployed, they remain energy-intensive and unable to treat high salinity water sources. In the context of fit-for-purpose water, there is a great need for new technologies to treat a

Water classification	Salinity (weight%)	Salinity (ppm)	Use	MSF	MED	RO	DSE
Freshwater	0-0.10%	0-1,000 ppm	Human consumption, livestock and irrigation	✓	✓	✓	✓
Slightly saline water	0.10-0.16%	1,000-1,600 ppm	Livestock, may require special treatment for irrigation	✓	✓	✓	✓
	0.16-0.30%	1,600-3,000 ppm	Poultry and pigs	✓	✓	✓	✓
Moderately saline water	0.30-1.00%	3,000-10,000 ppm	Suitable for cattle or sheep and for flushing toilets	✓	✓	✓	✓
Very saline water	1.00-3.50%	10,000-35,000 ppm	Industrial usage(2%), thermoelectric power plants (95%) and mining (3%)	✗	✗	✓(partially)	✓
Briny water	>3.50%	>35,000 ppm		✗	✗	✗	✓

Table 1: Natural and man made sources of water range from freshwater (0-0.10% salinity) to briny water (>3.50% salinity) [1]. Salinity requirements vary widely depending on end use. For example, low salinity water is used for human and livestock consumption. But high salinity water with more than 35,000 ppm is suitable for industrial uses including power plant cooling and mining. While well-established technologies including Multi-stage Flash (MSF), Multi-effect Desalination (MED) and Reverse Osmosis (RO) have greatly advanced desalination industry [11], there remains a need for sustainable and energy efficient process to treat high salinity water. Directional Solvent Extraction (DSE) has been proven to be able to treat high salinity brines while utilizing low-grade heat.

wide range of water quality levels in distributed networks while using renewable energy.

Directional solvent extraction (DSE) uses a thermoresponsive solvent to facilitate treatment over a wide salinity range [13]. DSE does not require membranes, which often foul at high salinities, and can utilize low-grade heat, including waste or renewable (solar) sources. Prior work in DSE includes characterization of molecular phenomena, bench-scale demonstrations, and limited process analysis [14, 15, 13, 16, 17, 18]. This paper presents a techno-economic optimization framework with two new capabilities: first, we perform simultaneous process optimization and heat integration to rapidly screen directional solvent candidates in seconds. Second, we perform a sensitivity analysis to identify the necessary solvent properties to enable cost-effective DSE processes for a specific application. We emphasize these advances in process-scale models can rapidly accelerate DSE development by reducing the need for expensive experiments and guiding (computational) molecular design. To our knowledge, this is the first application of equation-oriented process optimization to facilitate bottom-up and top-down analysis of the DSE process.

The remainder of this paper is organized as follows. Section 2 reviews literature on desalination and DSE, with an emphasis on the scope for optimization.

Section 3 describes the optimization framework and mathematical models. Section 4 studies the impact of heat source temperature and solvent properties on the optimized process's minimum specific energy. Section 5 presents quantitative solvent property goals to achieve \$0.50/m^3 LCOW target for two classes of molecules: carboxylic acids and ionic liquids. Finally, Section 6 summarizes conclusions, limitations, and future work.

3. Literature review

3.1. Desalinaton technologies

Modern desalination technologies, including evaporative and reverse osmosis systems, are energy-intensive and not suitable to treat high salinity water. Evaporative systems such as multi-stage flash (MSF) and multi-effect distillation (MED) utilize thermal energy (typically 90°C and 55°C, respectively) to evaporate and condensate water [7]. These systems require highly corrosion-resistant and costly materials [19] and are heat-intensive (26.29-83.06 kWh/m^3); they require three or four times the theoretical minimum energy of separation [8, 7]. In contrast, membrane-based technologies such as reverse osmosis (RO) use mechanical work to overcome the osmotic pressure across a membrane. Membrane-based technologies use significant electricity inputs, need frequent membrane replacement, and have limited effectiveness when treating concentrated brines [8]. New technologies, including electrodialysis and forward osmosis, show promise to reduce energy consumption and lower costs. For example, osmotically assisted reverse osmosis (OARO) and mechanical vapor compression (MVC) are suitable to treat high salinity brines (140,000 ppm and 150,000 ppm respectively) [20, 21, 22]. Nevertheless, MVC energy consumption is high (single-effect MVC 2342kWh/m^3, double-effect MVC 20kWh/m^3) [22]. OARO, RO, and other membrane-based technologies are often susceptible to membrane fouling at high salt concentrations [23]. While hybrid desalination systems paired with renewable energy sources are well-studied [24, 25, 26], there is limited work of technologies suitable for high salinity brines.

Table 2: Comparison of energetics, costs, and limitations of common desalination technologies [7, 23].

Technology	Multi-Stage Flash (MSF)	Multi-Effect Distillation (MED)	Reverse Osmosis (RO)
Specific energy	26.29-83.06 kWh/m^3	26.29-76.26 kWh/m^3	3.05-8.33 kWh/m^3
Thermal input temperature	90 °C	55-70 °C	ambient
Global deployment	8%	27%	60%
Cost	0.27-1.49 \$/m^3	0.80-1.50 \$/m^3	0.45-1.62 \$/m^3
Thermal energy input	High	High	Low
Electric energy input	Low	Low	High
Equipment size	Large	Large	Small
Membrane replacement or fouling	No	No	Yes

3.2. Directional Solvent Extraction

Directional solvent extraction can overcome limitations of thermal and membrane-based systems by efficiently separating high salinity feeds with low-grade waste heat (40 - 80 °C). DSE exploits thermoresponsive solvents that extract water from salty mixtures at elevated temperatures and release water (phase separate) when cooled. Directional Solvents (DS) have several features: (1) water can dissolve in the solvent, and the solubility increases with temperature; (2) the solvent is virtually insoluble in water; (3) the solvent does not dissolve salts. The DSE process, which is explained in Figure 1, is based on liquid-liquid extraction; the solubility of water in the directional solvent as temperature increases (thermoresponsiveness), which enables simple regeneration. These features give DSE several distinct advantages compared to existing technologies: (1) DSE is membrane-free and thus is not restricted by membrane fouling concerns for high salinity water; (2) DSE operates in the liquid state, which reduces the size and complexity of the equipment; (3) DSE can be paired with a low-temperature renewable heat source (e.g., low-cost thermal solar).

Amines [27] and alcohols [28] were explored over fifty years ago as the first directional solvents for desalination. These solvents can only treat low salinity water (5000 ppm) and have a high solubility in water, leading to high solvent losses [29]. In the 1990s, The Puraq Company proposed a liquid polymers-based [30, 31] directional solvent, which was commercially unsuccessful due to elevated solvent production costs [32], although recent work by Thanaplan *et al.* [33]

reexamines the energetics of the Puraq Company's process. Recently, Luo and co-workers proposed fatty acids, including decanoic acid ($CH_3(CH_2)_8COOH$) and octanoic acid ($CH_3(CH_2)_6COOH$) as directional solvents. The highly polar C=0 and O−H groups in the fatty acids facilitate the formation of hydrogen bonds with water molecules, which enables carboxylic acids to dissolve water. However, the chain end is hydrophilic, which helps ensure the solubility of the acids in water is negligible (30 - 150 ppm) [15]. In recent work, Guo *et al.* [34] proposed the use of ionic liquids, which have a greater thermoresponsivness ability compared to fatty acids. In this work, we will assess the technoeconomic potential of fatty acid and ionic liquid directional solvents in the context of an optimized DSE process.

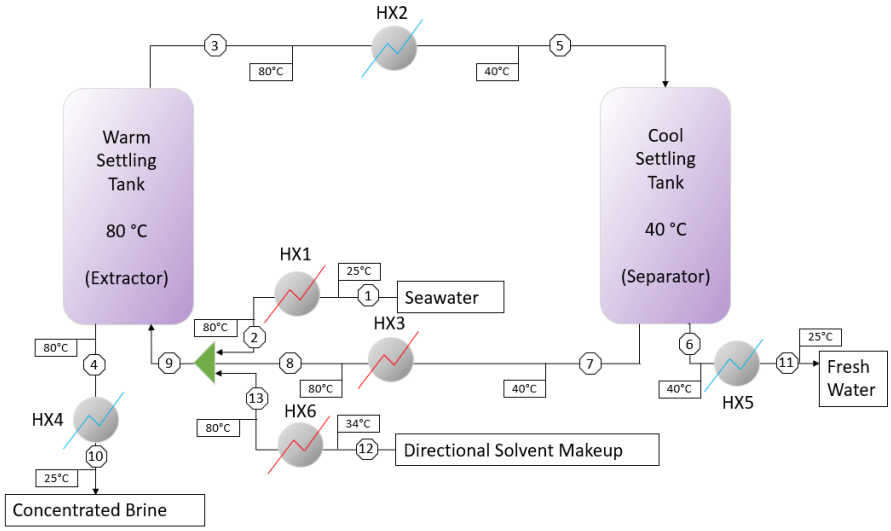

Figure 1: Illustration of the basic directional solvent extraction (DSE) process. Seawater (stream 1) is heated to the maximum allowable temperature (80°C is shown) in the process and mixed with the directional solvent (stream 8). The mixed emulsion of water and directional solvent (stream 9) settles in the warm settling tank. Water dissolves in the directional solvent, and concentrated brine (stream 4) is extracted from the mixture by gravity. The directional solvent and dissolved water (stream 3) are then cooled down. Freshwater is expelled from the mixture and decanted (stream 6). Decanoic acid is reheated and recycled (stream 8). A small amount of directional solvent dissolves in the freshwater and is lost (stream 6). Thus a small directional solvent make-up feed is added to the system (stream 12) to ensure steady-state operation.

3.2.1. Effectively utilize low-grade heat and no/limited membrane costs

Luo and co-workers [14, 15, 13, 16, 17, 18] recently demonstrated octanoic and decanoic acid can efficiently desalinate water. Specifically, they experimentally observed the solubility of water in decanoic acid changes from 3.8 wt% at 34°C to 5.9% at 80°C, with negligible solubility of fatty acid in water [16]. This thermoresponsive characteristic of the directional solvent enables thermal regeneration and is essential to the DSE process. Luo and co-workers then demonstrated the DSE concept in a continuous bench-scale process, successfully extracting 2.5 gallons of freshwater per day from a 700 ppm to 1100 ppm salinity feed (0.07-0.11 wt%) utilizing octanoic acid [16]. Based on these experi-

ments, they estimated a total energy consumption of 184 kWh/m^3 for decanoic acid and 101 kWh/m^3 for octanoic acid, assuming heat integration with 90% heat exchanger efficiency[16].

3.2.2. Demonstrated performance for higher salinities

Bajpayee *et al.* [14] demonstrated the effectiveness of octanoic acid to treat salty brines from 3,667 ppm to 58,333 ppm TDS (total dissolved solids). Likewise, they successfully treated saturated brines show water extraction with DSE of brine with 290,000 ppm (NaCl) [14]. These results are promising for DSE to treat produced water with high TDS from oil and gas extraction (up to 460,000 ppm).

3.2.3. Scope for molecular-to-systems optimization

There are vast unexplored opportunities to optimize DSE across molecular and process scales. Existing fatty solvents require ≈90 m^3 of recycle per 1 m^3 of freshwater, which makes the processes remain energy-intensive. Alotaibi *et al.* [16] performed heat integration for a single-stage continuous process for DSE utilizing octanoic and decanoic acids using flowrates obtained from bench-scale experiments [16]. Their analysis used the transshipment heat integration model, which assumes fixed flowrates and temperatures [35]. While insightful, this analysis technique often overlooks opportunities to reduce energy intensity that are only realizable by simultaneously optimizing process conditions (flowrates, temperatures, compositions) and performing heat integration [36]. In this work, we show the benefits of more extensive process optimization. At the molecular scale, Guo *et al.* [34] recently measured the thermophysical properties of a handful of ionic liquids as candidate directional solvents. However, there are well over a billion candidate solvents to consider. In this work, we use rigorous process modeling and optimization to set quantitative solvent thermophysical property targets as a means to narrow the vast molecular design space.

4. Methods: technoeconomic optimization framework

As a first step to realize molecular-to-system optimization of the DSE platform, we propose a computational framework for bottom-up rapid screening of candidate solvent and top-down identification of continuous solvent properties. In this section, we fully define the mathematical models and computational implementation.

4.1. Problem statement

Given inlet water salinity (e.g., 35,000 ppm NaCl), water rejection ratio (e.g., 50% water rejection rate), physical properties of the directional solvent, and a maximum temperature of the heat input, *manipulate* the temperature and material flows in the DSE process (streams in Figure 1) to *minimize* the specific energy of the problem. We formulate this as a nonlinear optimization problem (M1):

min	Specific Thermal Energy	
s.t.	Unit Operation Models	Table 3
	Embedded Heat Integration	Eq. (4)-(10)
	Physical Bounds	
	50% Water Rejection Rate	
	Inlet Water Specification (Seawater)	

We use variations of the optimization problem (M1) for both bottom-up screening and top-down analysis. We adopt an equation-oriented (EO) approach, wherein all of the process specifics and governing engineering phenomena (e.g., thermodynamics, equipment performance, energy costs, etc.) are expressed as mathematical equations that are simultaneously converged during optimization. This approach is extremely flexible. It naturally accommodates variable bounds and facilitates embedded heat integration during the optimization procedure. (M1) is a nonconvex optimization problem with 77 linear equality constraints, 26 nonlinear equality constraints, 6 linear inequality constraints,

6 nonlinear equality constraints, 30 quadratic equality constraints, and 136 variables. Using the Julia [37] and JuMP [38] computational environment, we can efficiently solve (M1) using IPOPT solver [39] and HSL (MA27) [40] in approximately 0.2 seconds after thoughtful initialization. The remainder of this section describes all of the mathematical equations and input data used in (M1).

4.2. Unit Operation Models

The DSE process is a collection of tanks, heat exchangers, splitters, and mixers, as shown in Figure 1, connected by thirteen streams contained in set $\mathcal{S}$. Variables flowrate F and temperature T are indexed by set $\mathcal{S}$. The mole fraction variable is indexed by the set of streams ($\mathcal{S}$) and the set of components ($\mathcal{C}$) which includes the directional solvent, water, and salt. Mass and energy balances and liquid-liquid equilibria equations, which as shown in Table 3, are used to relate these variables for inlet and outlet streams. We assume the entire process operates at a steady-state and there are no chemical reactions.

Table 3: Each unit operation is modeled as a collection of equations that relate the inlet and outlet streams. The following variables are indexed over the set of streams $\mathcal{S}$: the molar flow F (kmol/s), the temperature T (K), and the heat capacity C_p (J/mol-K). The molar fractions x are indexed over both $\mathcal{S}$ and the components $\mathcal{C}$ which include the solvent, water, and salt. The sets $\mathcal{I} \subset \mathcal{S}$ and $\mathcal{O} \subset \mathcal{S}$ are the inlet and outlet streams of each unit operation. For simplicity, the index *in* or *out* is used if there is only one inlet or outlet, respectively. The settling tank outlets have indices o_1 and o_2 for the aqueous and solvent phases, respectively, such that $\{o_1, o_2\} = \mathcal{O}$. We assume salt has a fixed solubility of κ_s (mole fraction) in the solvent phase and the directional solvent has a fixed solubility of κ_d (mole fraction) in the aqueous phase.

Equation	Tanks	Isothermal mixer	Single phase heat exchanger
Overall mass balance	$F_{in} = \sum_{j \in \mathcal{O}} F_j$	$\sum_{i \in \mathcal{I}} F_i = F_{out}$	$F_{in} = F_{out}$
Overall component balance	$F_{in} x_{in,c} = \sum_{j \in \mathcal{O}} F_j x_{j,c} \quad \forall c \in \mathcal{C}$	$\sum_{i \in \mathcal{I}} F_i x_{i,c} = F_{out} x_{out,c} \quad \forall c \in \mathcal{C}$	$x_{in,c} = x_{out,c} \quad \forall c \in \mathcal{C}$
Chemical equilibrium	Water: $x_{o_1,w} = A + BT_{o_1}$ Salt: $x_{o_1,s} = \kappa_s$ Directional Solvent: $x_{o_2,d} = \kappa_d$		
Summation equation	$\sum_{c \in \mathcal{C}} (x_{o_1,c} - x_{o_2,c}) = 0$		
Energy Balance	$T_{in} = T_{o_1} = T_{o_2}$	$T_i = T_{out} \quad \forall i \in \mathcal{I}$	$Q = C_p F_{in} (T_{out} - T_{in})$

4.2.1. Liquid-liquid phase separation

The DSE process relies on temperature varying solubility of water in the directional solvent. Unfortunately, temperature-dependent ternary phase data for water, solvent, and salt are not available in the literature. For preliminary process analysis, we assume the solubility of water in the solvent is linearly dependent on temperature shown in Eq. (1). We fit A and B via regression analysis using experimental data for the mixture decanoic acid, water, and salt from Bajpayee *et al.* [14] and Oliveira *et al.* [41] for the mixture decanoic acid and water. Figure 2 shows this simple model fits the data well. Fitted parameters are reported in Table 4. We assume the direction solvent has a fixed solubility in the aqueous phase, denoted κ_d. Values are given in Table 5. Likewise, we assume salt has a fixed solubility of $\kappa_s = 65$ ppm (0.0199 mol/mol) in the solvent

phase.

$$x_w = A + BT \tag{1}$$

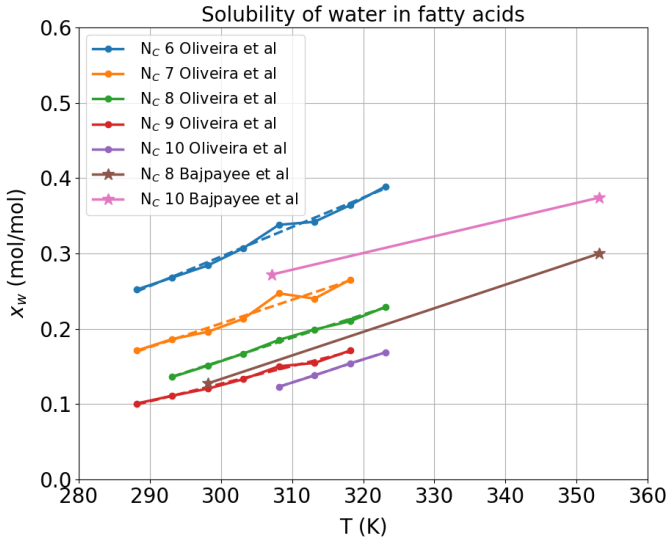

Figure 2: We perform linear regression on solubility to calculate the temperature swing (thermoresponsiveness) of the solubility of water in the carboxylic acid (solvent phase) using two sets of experimental data. Bajpayee *et al.* [14] provides data for ternary mixtures C_8 and C_{10} fatty acids, water, and salt. Oliveira *et al.* [41] provides data for binary mixtures of C_6 to C_{10} fatty acids and water.

Table 4: Coefficients for the equation $x_w = A + BT$ for solubility correlation for carboxylic acids and [emim][Tf_2N][34].

Bajpayee *et al.* [14]

Number of carbons	**A (mol/mol)**	**B (mol/mol K)**
8	-0.8304	0.0032
10	-0.4091	0.0022

Oliveira *et al.* [41]

Number of carbons	**A (mol/mol)**	**B (mol/mol K)**
6	-0.5731	0.0039
7	-0.7618	0.0031
8	-0.7367	0.0031
9	-0.5743	0.0023
10	-0.8187	0.0036
Ionic liquid	**A (mol/mol)**	**B (mol/mol K)**
[emim][Tf_2N]	-1.3417	0.0063

Table 5: Solubility of carboxylic acids and ionic liquid in water [42, 34].

Acid	**N_c**	**Solvent solubility in water (mol/mol)**	**Solubility in water [ppm]**
Hexanoic	6	1.678E-3	10,820
Heptanoic	7	3.348E-4	2,419
Octanoic	8	8.495E-5	680
Nonanoic	9	3.416E-5	300
Decanoic	10	1.339E-5	128
Ionic Liquid		**Solvent solubility in water (mol/mol)**	**Solubility in water [ppm]**
[emim][Tf_2N]		5.985E-6	300

4.2.2. Single-phase heat exchanger

The heat duty in the heat exchanger is $Q = C_p F_{in}(T_{out} - T_{in})$, where C_p is the heat capacity, F_{in} is the flowrate, and $T_{out} - T_{in}$ is the temperature difference. We calculate C_{pi} for the organic solvent i with the capacity group

contribution method [43]:

$$C_{pi} = \sum_{k \in \mathcal{G}} N_k (A_k + B_k t) \qquad t = T/1000 \tag{2}$$

Eq. (2) captures the influence of N_k times of functional group k appears in the organic component i. For water we use coefficients given in Table 7[43]:

$$C_{pi} = A + Bt + Ct^2 + Dt^3 + E/t^2, \qquad t = T/1000 \tag{3}$$

and for the ionic liquid, we use coefficients given in Table 7 and Eqs. (4) [44].

$$C_{pi} = A + BT \tag{4}$$

We then calculate the C_p of each stream (mixtures) using the the component heat capacities C_{pi} and the mole fractions x_i:

$$C_p = \sum_{i \in C} C_{pi} x_i \tag{5}$$

The heat capacity of NaCl is considered constant with a value of 15.058 J/mol-K [43]. Coefficients for Eqs. (2)-(4) are given in Tables 6 and 7.

Table 6: Heat capacity parameters for group contribution method [43].

Functional group	**A**	**B**
	J/molK	J/mol-K^2
CH_3	14.5504	540.60
CH_2	19.539	32.21
COOH	-49.7595	421.11

4.3. Embedded Heat Integration

We embed the Duran-Grossman heat integration equations [45] directly into the process optimization problem. This allows us to simultaneously optimize the

Table 7: Heat capacity parameters for Eq. (3) [43] and Eq. (4) [44]. $C_{pi} = A + Bt + Ct^2 + Dt^3 + E/t^2$, $t = T/1000$ (J/mol-K).

Component	**A**	**B**	**C**	**D**	**E**
	(J/mol-K)	(J/mol-K*kK)	(J/mol-K*kK^2)	(J/mol-K*kK^3)	(JkK^2/molK)
H_2O	-203.6060	1583.29	- 3196.43	2474.455	3.855326
[emim][Tf_2N]	430.39	0.315	0	0	0

process operating conditions (flowrates, compositions, temperatures) while minimizing the thermal energy input per unit of freshwater product. In contrast, Alotaibi *et al.* [16] only perform heat integration for a fixed process operating conditions. We emphasize our approach is superior because it optimizes more degrees of freedom. The optimizer manipulates flowrates, compositions, and temperatures to balance complex interdependencies between temperature-dependent phase equilibria and the pinch point which limits heat integration. For completeness, we now summarize the heat integration model.

Each single-phase heat exchanger half is designated as a hot stream (requires cooling) or a cold stream (requires heating), denoted with sets $\mathcal{S}_\mathcal{H}$ and $\mathcal{S}_\mathcal{C}$, respectively. We then consider the inlet of each heat exchanger as a pinch candidate temperature T^p and add the minimum driving force ΔT_{min} to the cold stream temperatures:

$$T^p = \begin{cases} T_p^{in} & \forall \quad p \quad \in \mathcal{S}_\mathcal{H} \\ T_p^{in} + \Delta T_{min} & \forall \quad p \quad \in \mathcal{S}_\mathcal{C} \end{cases} \tag{6}$$

We use the set $\mathcal{P} = \mathcal{S}_\mathcal{C} \cup \mathcal{S}_\mathcal{H}$ to denote all pinch candidate temperatures. For each pinch candidate $p \in \mathcal{P}$, we calculate the heat content above pinch temperature T^p:

$$QA_H^p = \sum_{i \in \mathcal{S}_\mathcal{H}} FC_{pi}[\tilde{\max}(T_i^{in} - T^p) - \tilde{\max}(T_i^{out} - T^p)], \quad \forall p \in \mathcal{P} \tag{7}$$

Similarly, we calculate the heat content below pinch temperature T^p:

$$QA_C^p = \sum_{i \in \mathcal{S}_\mathcal{C}} FC_{pi}[\tilde{\max}(T_j^{out} - T^p + \Delta T_{min}) - \tilde{\max}(T_i^{in} - T^p \Delta T_{min})], \quad \forall p \in \mathcal{P} \tag{8}$$

The minimum hot utility duty Q_S must be larger than the difference between the heat contents below and above each pinch candidate.

$$\underbrace{Q_S}_{\text{heating utility}} \geq \underbrace{QA_C^p}_{\substack{\text{heat content above} \\ \text{pinch candidate}}} - \underbrace{QA_H^p}_{\substack{\text{heat content below} \\ \text{pinch candidate}}} \quad \forall \quad p \in \mathcal{P} \tag{9}$$

Finally, we use an energy balance to calculate the minimum cold utility duty Q_W:

$$\underbrace{Q_W}_{\text{cooling utility}} = \underbrace{Q_S}_{\text{heating utility}} + \underbrace{\sum_{j \in \mathcal{S}_C} Q_j^{in}}_{\text{internal heating}} - \underbrace{\sum_{i \in \mathcal{S}_H} Q_i^{out}}_{\text{internal cooling}} \tag{10}$$

To ensure optimization problem is differentiable, we use a smoothed approximation for the max operator:

$$\tilde{\max}(x) = \frac{1}{2}\left(\sqrt{x^2 + \epsilon^2}\right) \approx \max(x, 0), \qquad \epsilon^2 = 10^{-6} \tag{11}$$

This model is effective because the combinatorial search for the pinch candidate is cast as inequality constraint Eq. (9), which is efficiently handled in equation oriented process optimization.

4.4. Cost model

After solving (M1), we estimate equipment and operating costs and then calculate the price per unit of freshwater production.

The heat integration model described above only computes the minimum hot and cold utilities when solving (M1). As a post-processing step, we perform sequential optimization to design the heat exchanger network. We first solve a mixed integer linear program to predict matches to minimize the number of heat exchangers. We then solve a nonlinear program to calculate the heat exchanger areas.[35, 36]. Finally, we use Guthrie's Method [36] to calculate the equipment costs. We use the present cost index of December 2018 (613.6) and a straight-line depreciation:

$$ADE = \frac{(CotA - SV)}{ULA} \tag{12}$$

Here, ADE is the Annual Depreciation Expense, $CotA$ is the cost of the assets, SV is the salvage value after the useful life of the plant (20% of the cost of the assets), and ULA is the estimated useful life of the plant. We assume a cost of electricity of 0.05 \$/kWh (average price of Texas, Oklahoma, Lousiana, New Mexico, Georgia, and Utah) [46]. We assume a 2 psi pressure drop every 100 feet, and the heigh of the tanks is calculated for every process solution for pumping electricity. We assume a cost of heating utilities of 2.778 \$/GJ from waste heat, a similar cost to solid waste, coal, or nuclear energy [47]. We assume the system has a useful life of 20 years for cost calculations, and we selected stainless steel for the material of the equipment because the plant handles saline brines and freshwater. The cost of decanoic acid is set to 12 \$/kg [48].

5. Results: Bottom-up Process Optimization

We now solve the optimization problem (M1) in several bottom-up case studies to predict the best possible performance of candidate directional solvents in a fully optimization process. We first compare our optimized reference design with Alotaibi *et al.* [16]. Then, we perform a sensitivity analysis to quantify the impact of ΔT_{min} (heat exchanger size) and the maximum temperature (heat source quality). Finally, we compare candidate organic acid solvents.

5.1. Reference Design for Decanoic Acid Directional Solvent

We set the temperature bounds between 34°C and 80°C, specify a 50% reject ratio, and set $\Delta T_{min} = 6$°C[1] to match Altoabi *et al.* [16]. Results from solving (M1) are shown in Tables 8, 9, 10 and Figure 3. From the results, we draw these observations:

Observation A1. A considerable portion of the decanoic acid (128 ppm) is solubilized in the outlet of freshwater and salty brine. We calculate that, at steady-state, the process requires 10^{-4} kmol/s of make-up directional

[1] Altoabi *et al.* [16] report a heat exchanger effectiveness of 90%, which we convert to ΔT_{min} = 6°C.

solvent. We emphasize this make-up was not considered by Alotaibi *et al.*[16], who based their process analysis on pseudo-steady-state experimental data.

Observation A2. Our approach finds the same pinch point, 50°C, as shown in Altoabi *et al.* [16].

Observation A3. Solving (M1) predicts specific (thermal) energy of 191 kWh_t/m^3 of freshwater with decanoic acid as a solvent, whereas Alotaibi *et al.* [16] 180 kWh_t/m^3 of freshwater. We highlight two differences that can explain our 9% larger specific energy: first, the addition of a feed (make-up) stream of decanoic acid. Second, we cool down the solvent-water emulsion stream to 34°C (limiting temperature due to solvent crystallization) in contrast to the 40°C used by Alotaibi *et al.* [16].

Observation A4. Solving the cost analysis for treating 1 m^3 of water results in a cost of \$3.31 $/m^3$ of freshwater. The cost is high compared to modern technologies: between \$0.27 $/m^3$ and \$1.62 $/m^3$ of freshwater. Solvent loss has a significant influence on the cost of DSE desalination.

Table 8: Stream results for reference design with decanoic acid as solvent using 80°C as maximum allowable temperature ΔT_{min}=6°C. See Figure 1 for schematics. Flowrates are comparable to Table 3 in Alotaibi *et al.* [16].

Stream	**Flow**	**Temperature**	x_d	x_w	x_s
	kmol/s	°C	%mol	%mol	%mol
1	0.5	25	0.00	98.89	1.11
2	0.5	80	0.00	98.89	1.11
3	1.81	80	63.18	36.78	10^{-4}
4	0.25	80	10^{-3}	97.97	1.99
5	1.81	34	63.18	36.78	10^{-4}
6	0.25	34	10^{-4}	99.78	0.21
7	1.56	34	73.33	26.66	10^{-4}
8	1.56	80	73.33	26.66	10^{-4}
9	2.06	80	55.50	44.22	0.26
10	0.25	25	10^{-3}	97.97	1.99
11	0.25	25	10^{-4}	99.78	0.21
12	10^{-4}	34	100	0.00	0.00
13	10^{-4}	80	100	0.00	0.00

Table 9: Heat exchanger sizes and temperatures for the reference design (decanoic acid as solvent, 80°C as maximum allowable temperature). More than 90% of the heating and cooling occurs in heat exchangers HX3 and HX2, respectively. This is due to the large amount of decanoic acid that must be recycled to a achieve an overall 50% extraction ratio. For practical considerations, one may choose not to add HX6 due to the low heat duty of the heat exchanger and the small flow of solvent.

Heat exchanger	**Stream**		**Temp (°C)**		**Q (kWh)**
	Inlet	Outlet	Inlet	Outlet	
HX1	S1	S2	25	80	2.09
HX2	S3	S5	80	34	-23.44
HX3	S7	S8	34	80	23.00
HX4	S4	S10	80	25	-1.045
HX5	S6	S11	34	25	-0.17
HX6	S12	S13	34	80	3.2E-3

Table 10: Heat integration results for the reference design. QA_h is the heat exchanged above the pinch temperature and QA_c is the heat below the pinch temperature. Both streams S3 and S4 are at the pinch temperature of 50°C.

Heat exchanger	**Exchanger Inlet**	**Type of Stream**	**QA_h (kWh)**	**QA_c (kWh)**	**QA_c-QA_h (kWh)**
HX1	S1	Cold	24.03	24.31	0.28
HX2	S3	Hot	0.01	3.12	3.11*
HX3	S7	Cold	20.77	23.88	3.10
HX4	S4	Hot	0.01	3.12	3.11*
HX5	S6	Hot	23.88	24.17	0.28
HX6	S12	Cold	20.77	23.88	3.10

* Pinch temperature

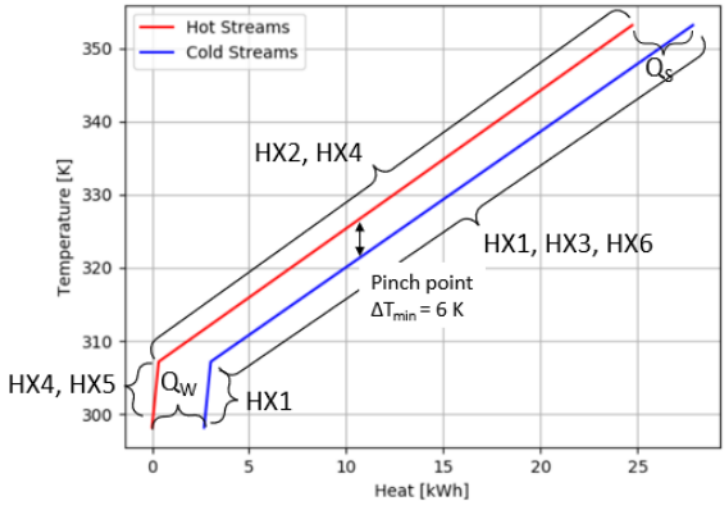

Figure 3: Composite curves for the reference design, including utilities. Most of the heat exchange is done in HX2 and HX3, which have the largest temperature difference and the highest flowrates. Recall HX1 heats inlet seawater to the temperature of the warm settling tank, HX2 cools the water-decanoic acid emulsion, and HX3 heats the recycled directional solvent. HX4 and HX5 cool the outlet concentrated brine and freshwater, respectively. Q_S and Q_W are defined as the minimum heating and cooling utility duties, respectively.

Table 11: LCOW for three different directional solvents without consifering solvent recovery. Costs of thermal energy, pumping electricity and equipment are lower using ionic liquid. However the cost of the solvent make-up increases considerably.

Directional solvent	LCOW	Solvent cost		Electricity cost		Thermal energy cost		Equipment cost	
	$	$	%	$	%	$	%	$	%
Decanoic acid	3.30	1.03	31.21	0.31	9.39	1.92	58.18	0.04	1.21
Octanoic acid	4.13	2.48	60.05	0.20	4.85	1.42	34.38	0.03	0.73
[emim][Tf_2N]	43.03	42.60	99.02	0.07	0.17	0.34	0.78	0.01	0.03

5.2. Sensitivity Analysis: Maximum Temperature and ΔT_{min}

Next, we considered the sensitivity of process designs to both the maximum temperature and ΔT_{min}, which controls the heat exchanger size and effectiveness. We solve (M1) with three different sets of experimental data as the LLE correlation input: decanoic acid-water data form Oliveira *et al.* [41], decanoic

acid-water-salt data from Bajpayee *et al.* [15], and [emim][Tf_2N]-water-salt data from Guo *et al.* [34]. Figure 4 shows specific energy at six maximum temperature between 40 °C and 90 °C and ten different ΔT_{min} between 1 °C and 10 °C. Figure 5 shows specific energy at five maximum temperature between 35 °C and 75 °C and ten different ΔT_{min} between 1 °C and 10 °C. Solving (M1) 169 times to generate Figures 4 and 5 took less than 1 minute. Table 12 gives the stream information for a single design from the sensitivity analysis (T_{max} =50°C, ΔT_{min} =6 °C). From these results, we observe:

Observation B1. We find consistent trends with both sets of solubility data. Bajpayee *et al.* data[15] showed 2.6% more solubility of water in the solvent phase, which leads to 2 times lower energy-intensive process as the process needs fewer extractions per pass. The difference between the solubilities is because Oliveira *et al.* only considered binary water-acid mixtures.

Observation B2. As expected, higher maximum temperatures enable higher per pass extraction, which allows for a lower recycle flowrate (1.81 kmol/s for T_{max}= 80°C versus 4.91 kmol/s for T_{max}=50°C) and lower energy intensity (191.84kWh_t/m^3 for T_{max}= 80°C verus 551.90kWh_t/m^3 for T_{max}=50°C). This suggests that manipulating the solvent chemistry to increase the per pass extraction at a lower temperature will decrease the energy intensity.

Observation B3. The specific energy difference between temperature ≤80°C and ≤90°C is negligible. This is because increasing the pass per extraction increases the fraction of water in the solvent-water emulsion, which decreases the C_p of the mixture. As the amount of heat required to heat the mixture decreases at a higher maximum allowable temperature, so does the specific energy of the process. This result emphasizes little benefit for heat sources greater than 80°C for off-the-shelf organic acid solvents.

Observation B4. Heat exchangers with a temperature difference of less than 3°C are likely required to achieve less than 50kWh_t/m^3 and 4°C to achieve less than 100kWh_t/m^3 utilizing decanoic acid as a solvent. The heat exchangers would need to have an effectiveness of approximately 96% or higher to achieve the 50kWh_t/m^3 goal utilizing decanoic acid.

Observation B5. We observe the IL the solvent [emim][Tf_2N] can achieve 50 kWh_t/m^3 using maximum allowable temperature of 65°C and ΔT_{min} of 6°C. Our analysis shows that, from an energetics perspective, ILs are a more promising class of directional solvents.

Table 12: Stream results for reference design with decanoic acid as solvent using 50°C as maximum allowable temperature ΔT_{min}=6°C. See Figure 1 for stream numbers.

Stream	**Flow**	**Temperature**	x_d	x_w	x_s
	kmol/s	°C	%mol	%mol	%mol
1	0.5	25	0.00	98.89	1.11
2	0.5	50	0.00	98.89	1.11
3	5.16	50	69.79	30.18	0.03
4	0.25	50	10^{-3}	98.41	1.58
5	5.16	34	69.79	30.18	0.03
6	0.25	34	10^{-4}	99.37	0.62
7	4.91	34	73.33	26.66	10^{-4}
8	4.91	50	73.33	26.66	10^{-4}
9	5.16	50	66.56	33.33	0.10
10	0.25	25	10^{-3}	98.41	1.58
11	0.25	25	10^{-4}	99.37	0.63
12	10^{-4}	34	100	0.00	0.00
13	10^{-4}	50	100	0.00	0.00

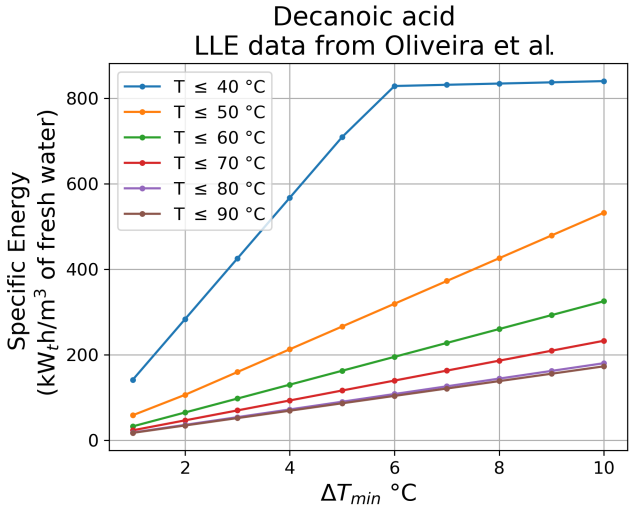

(a) Using data from Oliveira *et al.* [41]

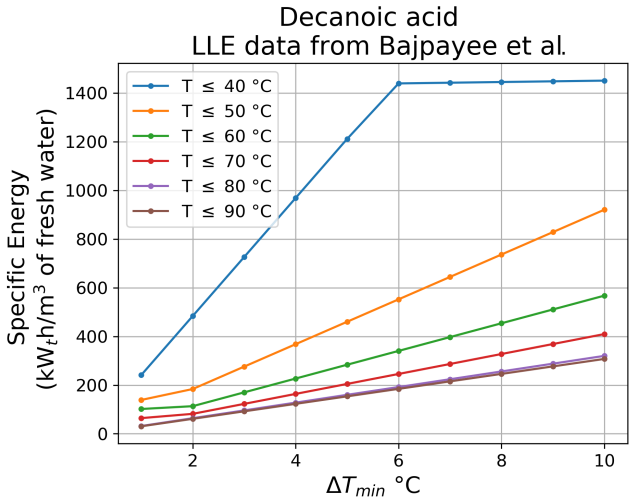

(b) Using data from Bajpayee *et al.* [15]

Figure 4: Sensitivity of specific energy to maximum temperature (heat source quality) and ΔT_{min} (heat exchanger size). Bajpayee *et al.* [15] data showed 2.6% more solubility of water in the solvent phase from Oliveira *et al.* [41]. The difference may be explained by the interaction of salt in the mixture. Higher maximum temperatures enable higher per pass extraction, which allows for a lower recycle flowrate and lower energy intensity. Solvents that enables higher per pass extraction at a lower temperature, the decrease in energy intensity would be higher. The specific energy difference between allowing (M1) to reach 80°C and 90°C is negligible. Heat exchangers with a temperature difference of less than 3°C are to achieve less than 50 $\mathrm{kWh_t/m^3}$.

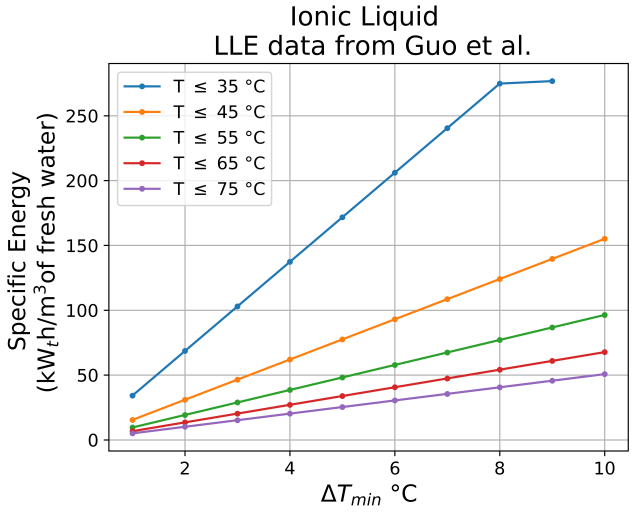

Figure 5: Effects of maximum temperature allowed for the process utilizing [emim][Tf_2N] as solvent. The specific energy of the process is greatly reduced compared to carboxylic acids.

5.3. Sensitivity Analysis: Length of the Chain of Carboxylic Acids

We now rapidly screen five carboxylic acids as directional solvents. We solve (M1) using acid-water mixture data for Oliveira *et al.* [41]. We set the amount of acid dissolved in the aqueous phase as the solubility of the fatty acid at 20°C, shown in Table 5. The minimum temperature for the process is set as the larger of the melting temperature of the acid or 25°C at ambient temperature. The 120 instances of (M1) shown in Figure 6 were solved in approximately 25 seconds total. From the results, we observe:

Observation C1. In Figure 2, we see there is not a clear relationship between the solubility of water in organic acid and the length of the carbon chain. However, we find the slope B, i.e., the thermoresponsiveness of solubility, is most influential on specific energy.

Observation C2. For solvent selection, the three most important factors are i) the change in water solubility for a fixed temperature change (thermoresponsiveness); ii) the melting temperature of the fatty acid, which limits the minimum operating temperature; and iii) the solubility of the directional solvent in freshwater.

Observation C3. Similar to observation B4, high-performance heat exchangers are required to achieve less than 50 $\mathrm{kWh_t/m^3}$ using $\mathrm{C_6}$ to $\mathrm{C_{10}}$ fatty acids

Observation C4. The cost of the process increases with the length of the carboxylic acid chain. The solvent solubility in water decreases as the carbon chain increases, diminishing the amount of solvent loss and the solvent make-up cost in the process.

Observation C5. DSE process using fatty acids are not economically viable, with a best-case scenario of \$1.29 per $\mathrm{m^3}$ of freshwater for decanoic acid with heat exchangers with ΔT_{min} of 1°C.

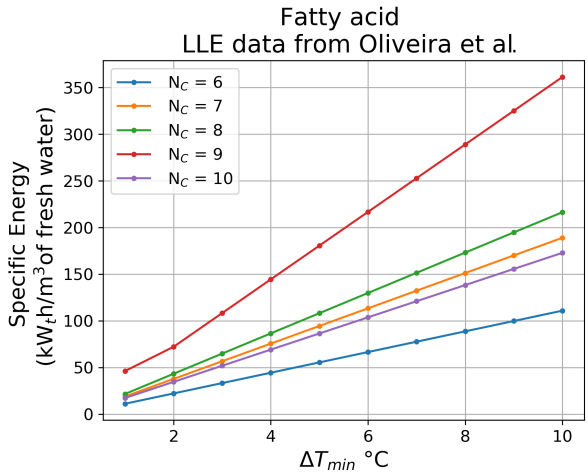

(a) Effects on specific energy using different carboxylic acids as the DS.

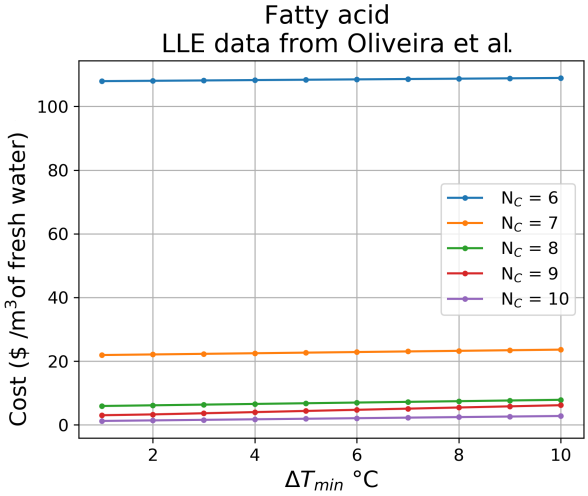

(b) Effects on the cost of the DSE process utilizing C_6 to C_{10} fatty acids.

Figure 6: There is not a clear influence in the length of the chain of carbons (N_c) in the energy required for the separation and the cost of the process. DSE remains energy intensive utilizing any C_6 to C_{10} carboxylic acid and suffers from solvent lost. The cost of the process increases with the increase of solubility of the solvent in water. The values of the cost at utilizing a ΔT_{min} from 1°C to°C 10 for different carboxylic acids are: for $N_c = 6$: \$107.91-108.99 per m^3, for $N_c = 7$: \$21.91-23.55 per m^3, for $N_c = 8$: \$5.90-7.86 per m^3, for $N_c = 9$: \$3.00-6.18 per m^3, for $N_c = 10$: \$1.29-3.79 per m^3. see Table 5 for specific quantities of solvent loss.

6. Results: Top-Down Solvent Property Targets

Based on the bottom-up analysis in Section 5, we conclude that known carboxylic acids are not an economical solution for directional solvent extraction. Although [emim][Tf_2N] is, from an energetic perspective, a more promising directional solvent, limited data for IL-water-salt mixtures prevents bottom-up screening of more candidate IL solvents.

In this section, we generalize the optimization problem (M1) to consider hypothetical directional solvent molecule parameterized by three continuous properties: solubilities in the aqueous and solvent phases and cost of the solvent. Thus we perturb four parameters in the technoeconomic analysis: A, B, solvent cost, and κ_d. We then perform top-down sensitivity analysis to identify **idealized directional solvent property targets** to add in molecular discovery. These continuous are a precursor to discrete molecular optimization [49].

6.1. Top-Down Analysis: Carboxylic Acids

We start by performing a sensitivity analysis for hypothetical carboxylic acid solvents over a grid for three properties: 1) the thermoresponsiveness of the solubility of the solvent (B), 2) the amount of water that solubilizes in the solvent at a reference temperature (A), and 3) the amount of solvent dissolved in the freshwater at the outlet of the DSE process (κ_d). Each candidate set of properties is first checked to ensure the solubility correlation Eq. (1) predicts a valid mole fraction between 0 and 1 at the process temperature bounds (T_{min} and T_{max}):

$$0 \leq A + BT_{max}, \quad 1 \geq A + BT_{max}, \quad 0 \leq A + BT_{min}, \quad 1 \geq A + BT_{min} \quad (13)$$

We found Eq. (13) is extremely effective at predicting if (M1) will be infeasible. For each set of properties that satisfy Eq. (13), we solve (M1) to compute flowrates and temperatures that minimize specific energy. For each solution of (M1), we estimate LCOW for a few solvent costs. From the results shown in Figure 7, we conclude:

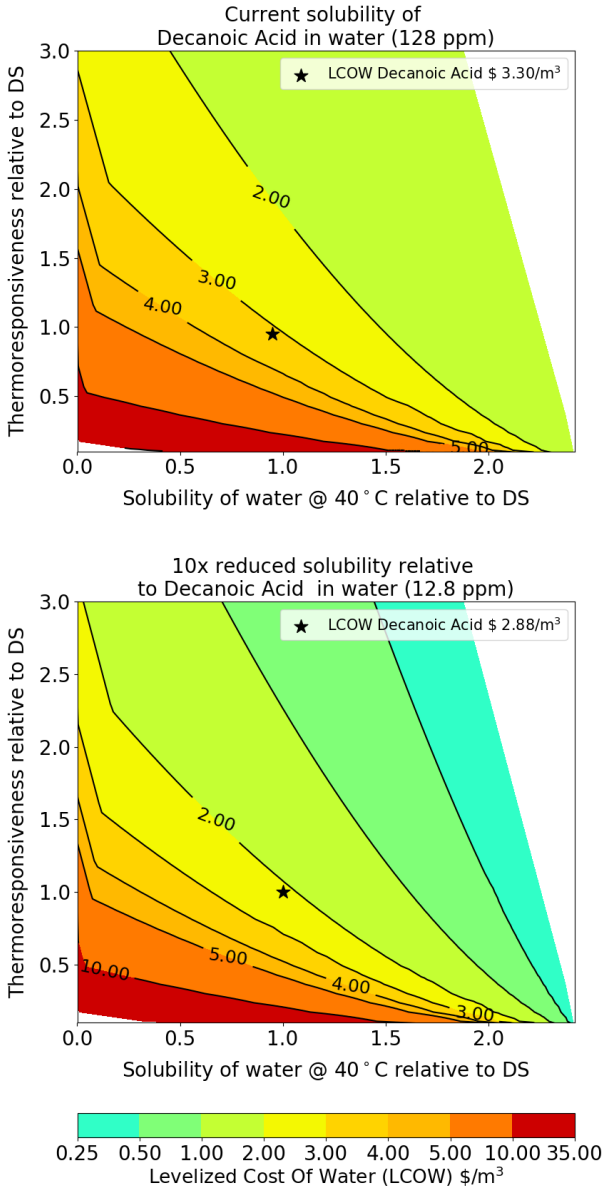

Figure 7: The colored contours show LCOW calculated using \$12/kg cost of decanoic acid as a function of thermoresponsivness (A, vertical axis) and the solubility of water at 40 °C(B, horizontal axis). Both axes are scaled such that 1.0, which is marked with a $\star$, corresponds to decanoic acid. (Top) Using the current solubility of the solvent in water (κ_d=128 ppm), a 2-fold improvement in both properties A and B result in a LCOW above \$1/m^3. (Bottom) Reducing the solubility of the solvent in water by 10-fold (κ_d=12.8 ppm) reduces the LCOW to \$2.88/m^3. Even with this improvement, A and B both need to increase by 1.5-fold to reach the \$0.5/m^3 LCOW goal.

Observation D1. For a directional solvent similar to a fatty acid, increasing thermoresponsive ability (B) and decreasing solubility of the solvent in water (κ_d) would cause the greatest reduction in LCOW. Likewise, increasing solubility of water in the solvent at a reference temperature (B) also reduces the recycle ratio by decreasing the amount of solvent needed for water to dissolve. We calculate LCOW of \$3.30/m^3 and \$4.13/m^3 for decanoic and octanoic acids, respectively. Even though energy contribution to LCOW is lower from octanoic acid (\$1.62/m^3 versus \$2.20/m^3), the overall LCOW is larger because the higher solubility of the solvent κ_d is larger (128 ppm for decanoic acid versus 300 ppm for octanoic acid), which causes larger solvent make-up costs (\$1.03/m^3 of freshwater for decanoic acid versus \$2.48/m^3 of freshwater for octanoic acid).

Observation D2. Figure 7 gives quantitive targets to reduce LCOW for a fatty acid-like directional solvent. For example, doubling the thermoresponsive ability (B) and reducing the solubility of the solvent in water by 10-fold (κ_d=128 ppm to 12.8ppm) relative to decanoic would give a LCOW less than \$0.50 /m^3.

Observation D3. The recycle ratio is reduced as the thermoresponsive ability (B) of the solvent and the base solubility of water in the solvent (A) increase. This reduces the thermal and electric energy required to heat, pump, and cool the recycle of the DSE-water emulsion. Reducing the recycle ratio also drastically shrinks the size of the equipment. For example, increasing the thermoresponsiveness of the solvent by a factor of 2 decreases the recycle ratio by a factor of 20, which decreases the heat and electricity costs from \$2.20 per m^3 of freshwater to \$0.21 per m^3 of freshwater, and decreases equipment sizes by 400%.

6.2. Top-down Analysis: Ionic Liquids

Next, we perform a sensitivity analysis for hypothetical IL directional solvents. Compared to carboxylic acids, ILs are a less mature chemical technology. We consider a current benchmark price of \$1,000/kg of [emim][Tf_2N] [50]. However, many expect economies of scale to dramatically reduce the cost of ILs as

the market for these solvents grows. For example, Shiflett *et al.* [51] shows a price reduction of 92% for $[C_2MIM]^+[Ace]^-$ and 90% for $[C_2MIM]^+[BF_4]^-$. For the sensitivity analysis, we consider three IL costs: \$1,000/kg, \$100/kg, and \$10/kg. Due to these comparatively high costs, solvent loss is especially important for ILs compared to carboxylic acids. Thus, it is desirable to consider solvent recovery systems, such as a membrane for post-treatment.[2] For simplicity, we consider the complete recovery of the solvent from the freshwater feed product, which can be recovered with a nanofiltration polishing step.

Observation E1. [emim][Tf_2N] is approximates 2 times more thermoresponsive (A) than decanoic acid (0.0063 mol/mol/°C vs. 0.0022 mol/mol/°C). However, at the current price of the ionic liquid, the solvent loss (κ_d) is critical. Figure 8 predicts that a ten-fold decrease in κ_d decrease LCOW to only 12% of the original cost. Improving the thermoresponsiveness (B) alone is insufficient for ILs to be LCOW-competitive with carboxylic acids. Assuming the current price of IL, the solvent would still require a 100 fold reduction of the solvent solubility ($x_{o_1,d}$).

Observation E2. Assuming a 90% cost reduction, the thermoresponsivness would need to be increased 1.5 times or the solubility of water 1.25 times. However, the solvent's solubility in water would need to be reduced by a ten-fold, as shown in Figure 8.

Observation E4. For a cost of [emim][Tf_2N] of \$10/kg, the solvent solubility in water would have to be 10 times lower, and the goal of \$0.50/m^3 of freshwater would be achieved. However, it would still be possible to reach the target goal by increasing 1.2 the solubility of water in the solvent or increasing 1.5 the thermoresponsiveness.

[2] IL recovery from the freshwater stream is achievable with off-the-shelf filtration systems. Post-treatment for the brine reject is much more challenging due to concerns of membrane fouling. Full costing of the freshwater post-treatment system is beyond the scope of this work. Instead, we neglect capital costs and energy usage. As such, the property targets are optimistic but informative.

Observation E5. For solvent with a cost as high as [emim][Tf_2N], the thermoresponsivness (B) and the solubility of water in the solvent (κ_d) are the most important properties. With the current solvent solubility data, one would need to reduce the solvent loss at least ten-fold for ILs to be LCOW-competitive, even with a solvent cost reduction of 99%.

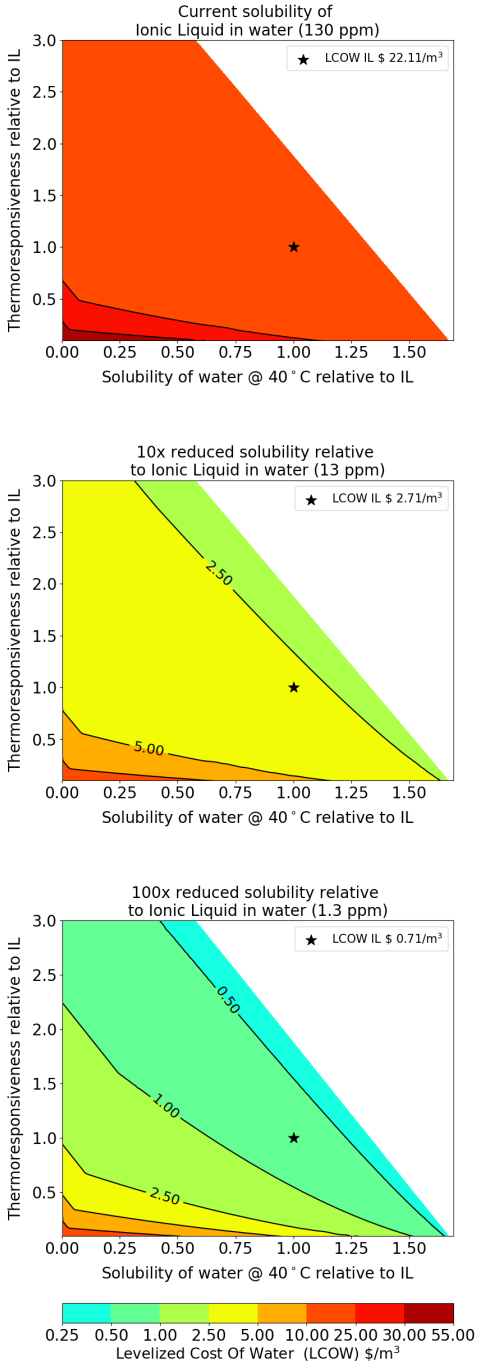

Figure 8: The colored contours show LCOW calculated using \$1,000/kg cost of [emim][Tf_2N] as a function of thermoresponsivness (A, vertical axis) and the solubility of water at 40 °C(B, horizontal axis). Both axes are scaled such that 1.0, which is marked with a $\star$, corresponds to [emim][Tf_2N]. Three scenarios for the solubility of IL in water κ_d are considered: (top) baseline, (middle) 10-fold decrease, and (bottom) 100-fold decrease.

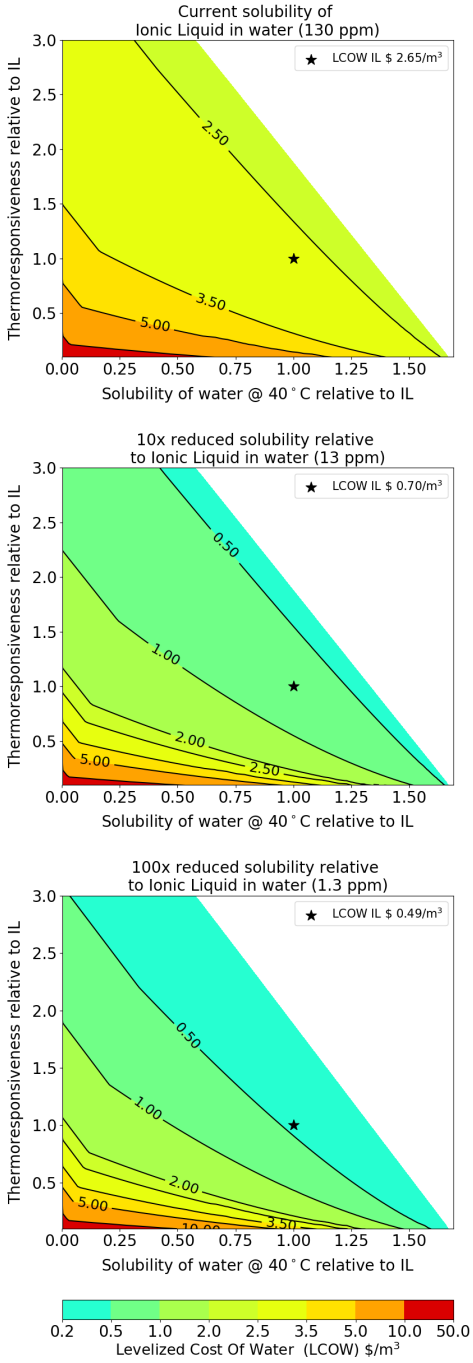

Figure 9: Colored contours show LCOW calculated using \$100/kg of [emim][Tf_2N]. (Top) Assuming κ_d=130 ppm, the solvent loss severely raises LCOW. (Bottom) Assuming a ten-fold decrease in κ_d, only a 1.25-fold increase in A or a 1.5-fold increase in B is needed to achieve a LCOW less than \$0.50/m^3. New unpublished data suggest these low solubility scenario is reasonable for a salty brine. (Bottom) A 100-fold decrease in κ_d alone gives a LCOW of \$0.49/m^3 under this low IL cost scenario.

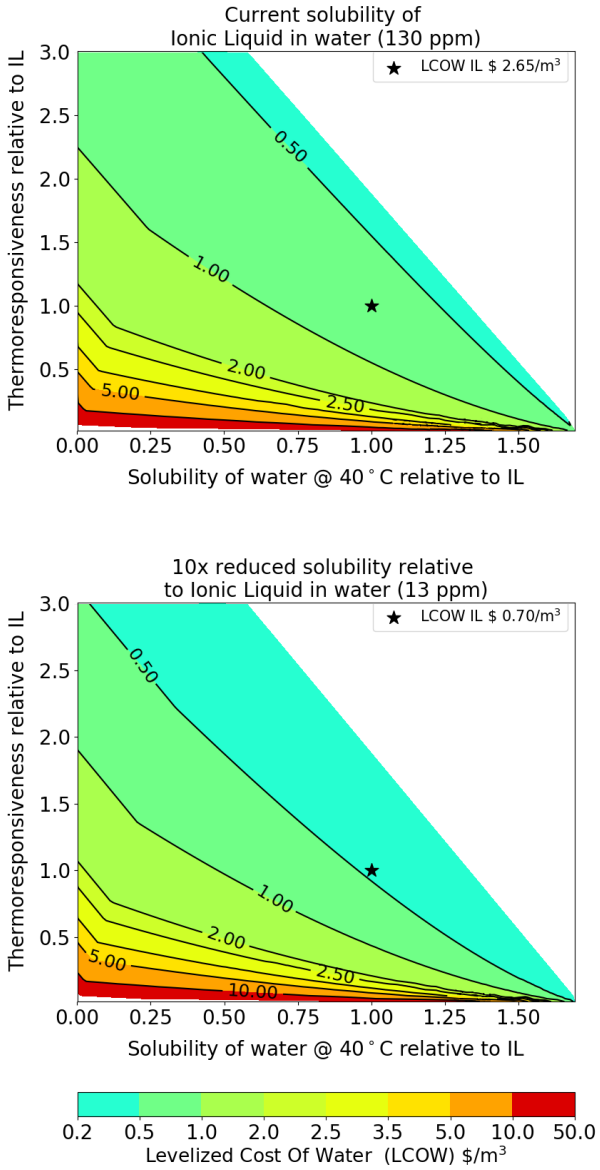

Figure 10: Sensitivy of LCOW with a cost of \$10/kg of [emim][Tf_2N]. (Top) With current solubility, the thermoresponsivness or the solubility of water would need to improve to achieve the required LCOW. (Bottom) With a 10 fold reduction of the solubility of the solvent in water we can achieve a LCOW of \$0.50/m^3 of freshwater.

7. Conclusions and Future Work

Directional solvent extraction is a membrane-free desalination technology that can treat high salinity water resources using low-grade heat. DSE can be paired with other technologies, e.g., renewable solar thermal collectors, to create hybrid sustainable systems. In this work, we created a computational framework that facilitates the optimization of the process and rapid sensitivity analysis. Through these analyses, we found that higher maximum temperatures enable higher per pass extraction, which allows for a lower recycle flowrate and lower energy intensity. For solvent selection, we found that the length of the carbon chain has no apparent influence and that the most critical factors are the change in water solubility for a low-temperature swing (40°C-80°C), the melting temperature of the fatty acid, which limits the minimum operating temperature and the solubility of DS in freshwater. Technoeconomic optimization was performed for five candidate fatty directional solvents ranging, giving LCOW predictions between $\$1.3/m^3$ and $\$109/m^3$. Sensitivity analysis shows significant improvements in three solubility properties are needed for the hypothetical fatty acid-like DS to achieve less than $\$0.5/m^3$. In contrast, ILs show much greater promise as directional solvents. Using newly published data from [emim][Tf_2N] and assuming a moderate solvent price of \$100/kg, we predict a modest $\$2.65/m^3$ LCOW. Sensitivity analysis shows the required combination of thermophysical properties necessary to achieve LCOW to below $\$0.5/m^3$. These results emphasize the potential of IL directional solvents.

As future work, we plan to explore process intensification opportunities (stage configuration, nanofiltration for solvent loss, electrocoalescer) and consider more detailed equipment models (nanofiltration to recovery solvent, electrocoalescer to replace settling tanks). Computer-aided molecular design (CAMD) approaches [52, 53, 54] offer promise to systematically search the billions of possible ionic liquids. We ultimately see computational molecular and process scale modeling greatly accelerated the search for economically viable directional solvents. We also plan to explore the opportunities and costs of coupling DSE with

inexpensive solar heating for sustainable and distributed desalination.

Nomenclature

	Sets and Elements
$\mathcal{C}$	Components
$d \in \mathcal{C}$	Directional solvent
$s \in \mathcal{C}$	Salt
$w \in \mathcal{C}$	Water
$\mathcal{G}$	Functional Groups
$CH_2 \in \mathcal{G}$	CH_2 functional group
$CH_3 \in \mathcal{G}$	CH_3 functional group
$COOH \in \mathcal{G}$	Carboxylic acid functional group
$H_2O \in \mathcal{G}$	Water
$\mathcal{N}$	Fatty Acid Directional Solvents
$6 \in \mathcal{N}$	Hexanoic acid
$7 \in \mathcal{N}$	Heptanoic acid
$8 \in \mathcal{N}$	Octanoic acid
$9 \in \mathcal{N}$	Nonanoic acid
$10 \in \mathcal{N}$	Decanoic acid
$\mathcal{S}$	Streams in Process
	See Figure 1 for stream numbers
$\mathcal{I} \subset \mathcal{S}$	Inlet streams (for a specific unit operation)
$\mathcal{O} \subset \mathcal{S}$	Outlet streams (for a specific unit operation)
$\mathcal{P} \subset \mathcal{S}$	Pinch candidates
$\mathcal{S}_\mathcal{C} \subset \mathcal{P}$	Cold streams
$\mathcal{S}_\mathcal{H} \subset \mathcal{P}$	Hot streams

Indices

$i \in \mathcal{C}$	Component
$k \in \mathcal{G}$	Functional group
$in \in \mathcal{I}$	Equipment inlet stream
$N_c \in \mathcal{N}$	Number of carbon atoms in fatty acid DS
$o_1 \in \mathcal{O}$	Solvent phase (tank effluent)
$o_2 \in \mathcal{O}$	Aqueous/salty phase (tank effluent)
$out \in \mathcal{O}$	Equipment outlet stream

Variables

A	Solubility of the solvent in water at a reference temperature
B	Thermoresponsiveness of the solubility of the solvent
C_p	Heat capacity (J/mol-K)
F	Molar flow (kmol/s)
Q	heat duty in the heat exchanger (kWh)
QA_C^p	heat content bellow pinch temperature (kWh)
QA_H^p	heat content above pinch temperature (kWh)
Q_S	Heat from hot utility (kWh)
Q_W	Heat from cold utility (kWh)
T	Temperature (K)
T^p	Pinch candidate temperature (K)
x	Molar fraction (mol/mol)

Parameters

κ_d	Fixed solubility of directional solvent in the aqueous phase (tank effluent) (mol/mol)
κ_s	Fixed solubility of salt in the solvent phase (tank effluent) (mol/mol)
ΔT_{min}	Heat recovery approach temperature (K)
T_{max}	Maximum allowable temperature of the process (°C)
T_{min}	Minimum allowable temperature of the process (°C)
N_C	Number of carbon atoms
N_k	Number of functional groups

Abbreviations

ADE	Annual Depreciation Expense
CotA	Cost of Assets
DS	Directional Solvent
DSE	Directional Solvent Extraction
IL	Ionic Liquid
LCOW	Levelized Cost of Water
MED	Multi-Effect Distillation
MSF	Multi-Stage Flash
MVC	Mechanical Vapor Compression
RO	Reverse Osmosis
OARO	Osmotically Assisted Reverse Osmosis
SV	Salvage Value
TDS	Total Dissolved Solids
ULA	Useful Life os Assets

References

[1] EPA, How we use water.
URL https://www.epa.gov/watersense/how-we-use-water#Daily%20Life

[2] M. M. Mekonnen, A. Y. Hoekstra, Sustainability: Four billion people facing severe water scarcity, Science Advances 2 (February) (2016) 1–7. doi:10.1126/sciadv.1500323.

[3] M. Kummu, J. H. Guillaume, H. De Moel, S. Eisner, M. Flörke, M. Porkka, S. Siebert, T. I. Veldkamp, P. J. Ward, The world's road to water scarcity: Shortage and stress in the 20th century and pathways towards sustainability, Scientific Reports 6 (December) (2016) 1–16. doi:10.1038/srep38495.

[4] UNDESA, International Decade for Action "Water for Life" 2005-2015.
URL https://www.un.org/waterforlifedecade/scarcity.shtml

[5] N. Voutchkov, Energy use for membrane seawater desalination current status and trends, Desalination 431 (2018) 2–14.

[6] L. Atkinson, L. Bass, Produced Water Report: Regulations, Current Practices, and Research Needs, Groundwater Protection Council.

[7] J. E. Miller, Review of water resources and desalination technologies, 2003-0800, Sandia National Laboratories (March) (2003) 1–54.

[8] M. Elimelech, W. A. Phillip, The future of seawater desalination: Energy, technology, and the environment, Science 333 (6043) (2011) 712–717. doi:10.1126/science.1200488.

[9] L. Yang, I. E. Grossmann, J. Manno, Optimization models for shale gas water management, AIChE Journal 60 (October) (2014) 3490–3501. doi:10.1002/aic.14526.

[10] L. Yang, R. Salcedo-Diaz, I. E. Grossmann, Water network optimization with wastewater regeneration models, Industrial & Engineering Chemistry Research 53 (45) (2014) 17680–17695. doi:10.1021/ie500978h.

[11] E. Jones, M. Qadir, M. van Vliet, V. Smakhtin, S.-m. Kang, The state of desalination and brine production: A global outlook, Science of The Total Environment 657 (2019) 1343–1356. doi:10.1016/j.scitotenv.2018.12.076.

[12] K. R. Zodrow, Q. Li, R. M. Buono, W. Chen, G. Daigger, L. Dueas-Osorio, M. Elimelech, X. Huang, G. Jiang, J.-H. Kim, B. E. Logan, D. L. Sedlak, P. Westerhoff, P. J. J. Alvarez, Advanced materials, technologies, and complex systems analyses: Emerging opportunities to enhance urban water security, Environmental Science & Technology 51 (18) (2017) 10274–10281. doi:10.1021/acs.est.7b01679.

[13] T. Luo, A. Bajpayee, G. Chen, Directional solvent for membrane-free water desalinationa molecular level study, Journal of Applied Physics 110 (5) (2011) Article 054905. doi:10.1063/1.3627239.

[14] A. Bajpayee, Directional Solvent Extraction Desalination (PhD thesis), Massachusetts Institute of Technology (MIT).

[15] A. Bajpayee, T. Luo, A. Muto, G. Chen, Very low temperature membrane-free desalination by directional solvent extraction, Energy Environ. Sci. 4 (2011) 1672–1675. doi:10.1039/C1EE01027A.

[16] S. Alotaibi, O. Ibrahim, S. Luo, T. Luo, Modeling of a continuous water desalination process using directional solvent extraction, Desalination 420 (2017) 114–124. doi:10.1016/j.desal.2017.07.004.

[17] S. Luo, J. C. Eng, P. Technol, S. Luo, Y. Pang, T. Luo, A Continuous Directional Solvent Extraction Desalination Process Realized with the Aid of Electro-coalescence, Journal of Chemical Engineering 9 (4) (2018) Article 1000392. doi:10.4172/2157-7048.1000392.

[18] S. Alotaibi, O. Ibrahim, Y. Wang, T. Luo, Exergy analysis of directional solvent extraction desalination process, Entropy 321 (2019) 321. doi:10.3390/e21030321.

[19] World Bank, The Role of Desalination in an Increasingly Water-Scarce World, World Bank, Washington, DC.doi:10.1596/31416.

[20] T. V. Bartholomew, L. Mey, J. T. Arena, N. S. Siefert, M. S. Mauter, Osmotically assisted reverse osmosis for high salinity brine treatment, Desalination 421 (2017) 3–11, the Latest Advances and Opportunities in Forward Osmosis. doi:10.1016/j.desal.2017.04.012.

[21] T. V. Bartholomew, M. S. Mauter, Computational framework for modeling membrane processes without process and solution property simplifications, Journal of Membrane Science 573 (2019) 682–693. doi:10.1016/j.memsci.2018.11.067.

[22] G. Thiel, E. Tow, L. Banchik, H. W. Chung, J. Lienhard, Energy consumption in desalinating produced water from shale oil and gas extraction, Desalination 366 (2015) 94–112. doi:10.1016/j.desal.2014.12.038.

[23] K. S. Spiegler, Y. M. El-Sayed, A Desalination Primer: Introductory Book for Students and Newcomers to Desalination, Balaban Desalination Publications, 1994.

[24] S. Loutatidou, H. A. Arafat, Techno-economic analysis of med and ro desalination powered by low-enthalpy geothermal energy, Desalination 365 (2015) 277–292. doi:10.1016/j.desal.2015.03.010.

[25] K. C. Ng, K. Thu, S. J. Oh, L. Ang, M. W. Shahzad, A. B. Ismail, Recent developments in thermally-driven seawater desalination: Energy efficiency improvement by hybridization of the med and ad cycles, Desalination 356 (2015) 255–270. doi:10.1016/j.desal.2014.10.025.

[26] R. S. El-Emam, I. Dincer, Thermodynamic and thermoeconomic analyses of seawater reverse osmosis desalination plant with energy recovery, Energy 64 (2014) 154–163. doi:10.1016/j.energy.2013.11.037.

[27] R. R. Davidson, W. H. Smith, D. W. Hood, Structure and amine-water solubility in desalination by solvent extraction., Journal of Chemical & Engineering Data 5 (4) (1960) 420–423. doi:10.1021/je60008a005.

[28] G. C. Johnson, Recovery of potable water from sea and brackish, U.S. Patent 3,823,000A.

[29] C. B. Ellis, N. D. A, Fresh water from the ocean for cities, industry, and irrigation, Ronald Press Co.

[30] L. Lazare, The puraq seawater desalination process, Desalination 42 (1) (1982) 11–16. doi:10.1016/S0011-9164(00)88736-6.

[31] L. Lazare, The puraq seawater desalination process - an update, Desalination 85 (3) (1992) 345–360. doi:10.1016/0011-9164(92)80016-3.

[32] Lack of money to develop solvent extraction desalting plant, Water Desalination Report 6 (2).

[33] K. Thanapalan, V. Dua, Using Low-Grade Heat for Solvent Extraction based Efficient Water Desalination, Vol. 29 of Computer Aided Chemical Engineering, Elsevier, 2011. doi:10.1016/B978-0-444-54298-4.50119-7.

[34] J. Guo, Z. D. Tucker, Y. Wang, B. L. Ashfeld, T. Luo, Task-Specific Ionic Liquid Enables Highly Efficient Low Temperature Desalination by Directional Solvent Extraction, chemrxiv.orgdoi:10.26434/chemrxiv.11840025.v1.
URL https://chemrxiv.org/articles/preprint/Task-Specific_Ionic_Liquid_Enables_Highly_Efficient_Low_Temperature_Desalination_by_Directional_Solvent_Extraction/11840025

[35] S. A. Papoulias, I. E. Grossmann, A structural optimization approach in process synthesis -ii: Heat recovery networks, Computers & Chemical Engineering 7 (6) (1983) 707–721. doi:10.1016/0098-1354(83)85023-6.

[36] L. Biegler, I. Grossmann, A. Westerberg, Systematic methods for chemical process design, Prentice Hall, 1997.

[37] J. Bezanson, A. Edelman, S. Karpinski, V. B. Shah, Julia: A fresh approach to numerical computing, SIAM review 59 (1) (2017) 65–98.

[38] I. Dunning, J. Huchette, M. Lubin, JuMP: A modeling language for mathematical optimization, SIAM Review 59 (2) (2017) 295–320. arXiv:1508.01982, doi:10.1137/15M1020575.

[39] A. Wächter, L. T. Biegler, On the Implementation of a Primal-Dual Interior Point Filter Line Search Algorithm for Large-Scale Nonlinear Programming, Mathematical Programming 106 (1) (2007) 25–57.

[40] "HSL. A collection of Fortran codes for large scale scientific computation. http://www.hsl.rl.ac.uk/".

[41] M. B. Oliveira, M. J. Pratas, I. M. Marrucho, A. J. Queimada, J. A. P. Coutinho, Description of the mutual solubilities of fatty acids and water

with the cpa eos, AIChE Journal 55 (6) (2009) 1604–1613. doi:10.1002/aic.11766.

[42] R. Battino, P. Seybold, Solubility correlations. part 1, Chemistry & Biodiversity 4 (11) (2007) 2547–2554. doi:10.1002/cbdv.200790208.

[43] NIST, National Institute of Standards and Technology[link].
URL https://www.nist.gov

[44] C. P. Fredlake, J. M. Crosthwaite, D. G. Hert, S. N. V. K. Aki, J. F. Brennecke, Thermophysical properties of imidazolium-based ionic liquids, Journal of Chemical & Engineering Data 49 (4) (2004) 954–964. doi:10.1021/je034261a.

[45] M. A. Duran, I. E. Grossmann, Simultaneous optimization and heat integration of chemical processes, AIChE Journal 32 (1) (1986) 123–138. doi:10.1002/aic.690320114.

[46] Year 2019 Industrial Firm Power Rates, Edison Electrical Institute.
URL https://www.consultbai.com/images/stories/publications/maps20_388251.pdf

[47] G. Ulrich, Chemical Engineering Process Design and Economics: A Practical Guide, Process Publishing, 2004.

[48] Foodchem International Corporation[link].
URL https://foodchem.cn

[49] A. Bardow, K. Steur, J. Gross, Continuous-molecular targeting for integrated solvent and process design, Industrial & Engineering Chemistry Research 49 (6) (2010) 2834–2840. doi:10.1021/ie901281w.

[50] Proionic[link].
URL https://www.proionic.com/bestseller/EMIM-TFSI-electronic-grade.php

[51] M. B. Shiflett (Ed.), Commercial Applications of Ionic Liquids, Springer, 2020.

[52] N. D. Austin, N. V. Sahinidis, D. W. Trahan, Computer-aided molecular design: An introduction and review of tools, applications, and solution techniques, Chemical Engineering Research and Design 116 (2016) 2–26, process Systems Engineering - A Celebration in Professor Roger Sargent's 90th Year. doi:10.1016/j.cherd.2016.10.014.

[53] R. Gani, Computer-aided methods and tools for chemical product design, Chemical Engineering Research and Design 82 (11) (2004) 1494 – 1504. doi:10.1205/cerd.82.11.1494.52032.

[54] L. Y. Ng, F. K. Chong, N. G. Chemmangattuvalappil, Challenges and opportunities in computer-aided molecular design, Computers & Chemical Engineering 81 (2015) 115 – 129. doi:10.1016/j.compchemeng.2015.03.009.